Quantitative Assessment of Mucosal Architecture Using Computer-Based Analysis of Confocal Laser Endomicroscopy in Inflammatory Bowel Diseases.

L Quénéhervé, G David, A Bourreille, Jean-Benoit Hardouin, G Rahmi, M Neunlist, J Brégeon, E Coron

Quantitative assessment of mucosal architecture using computer-based analysis of confocal laser endomicroscopy in inflammatory bowel diseases

Quénéhervé L[1,2*], M.D, David G[1,2*], M.D, Bourreille A[1,2], M.D, PhD, Hardouin JB[3], PhD, Rahmi G[4], M.D, PhD, Neunlist N[1,2*], PhD, Brégeon J[1,2*], PhD, Coron E[1,2*], M.D, PhD.

*Contributed equally to this work

[1]Université de Nantes, INSERM, IMAD, The enteric nervous system in gut and brain disorders, Université Bretagne Loire, Nantes, France

[2]Institut des Maladies de l'Appareil Digestif, IMAD, CHU Nantes, Hopital Hôtel-Dieu, Nantes, France

[3]Université de Nantes, INSERM, SPHERE, Université Bretagne Loire, Nantes, France

[4]Service d'Hépatogastroentérologie, Hôpital Européen Georges Pompidou, Paris

Word count: 3492/3500

Corresponding author:

Emmanuel Coron

Gastroenterology Unit

University Hospital of Nantes, Institut des Maladies de l'Appareil Digestif,

1 place Alexis Ricordeau 44000 NANTES, Tel.: +33 (0)2 40 08 31 52, Fax: +33 (0)2 40 08 31 54

emmanuel.coron@chu-nantes.fr

Abstract

Background and Aims: Confocal endomicroscopy (CLE) might discriminate mucosal lesions between Crohn's disease (CD) and ulcerative colitis (UC). However, the analysis of CLE images requires time-consuming methods, a long training time and potential impediments, such as significant interobserver variability. Therefore, we developed a computer-based method to analyze mucosal architecture from CLE images and discriminate between healthy subjects and patients with inflammatory bowel disease (IBD) as well as between UC and CD patients.

Methods: We retrospectively screened patients who had undergone CLE either for an evaluation of an IBD in remission or for colorectal cancer screening (controls) between 2009 and 2016. We assessed 14 morphological and functional parameters in each CLE recording from 23 CD patients, 27 UC patients and 9 control patients. Next, we constructed 2 scores, one for the IBD diagnosis (IBDiag) and the other for the differential diagnosis between UC and CD (IBDif).

Results: In IBD patients, the mean intercrypt distance, wall thickness and fluorescein leakage through the colonic mucosa were significantly increased compared with control patients by 155%, 188%, and 297%, respectively ($p<0.05$). In UC patients, the same parameters were significantly increased by 109%, 117%, and 174%, respectively ($p<0.05$), compared with CD patients. IBDiag had 100% [93%;100%] sensitivity and 100% [66%;100%] specificity. IBDif provided discrimination of UC from CD patients with 92% [75%;99%] sensitivity and 91%[72%;99%] specificity.

Conclusions: Confirming these results using prospective validation cohorts can substantiate that computer-based analysis of CLE images may provide new biomarkers for the diagnosis and the characterization of IBD.

Introduction

Confocal laser endomicroscopy (CLE) is an endoscopic technique for microscopic assessment of the gastrointestinal mucosa, which was introduced into clinical practice more than 10 years ago. CLE was initially used to detect neoplasia in a wide range of digestive cancers [1,2]. It was then gradually implemented for the evaluation of microscopic inflammation-linked abnormalities, particularly in inflammatory bowel diseases (IBD). In these patients, CLE was used, for example, to detect microscopic changes even in patients in remission [3,4]. However, analysis of CLE images remains

largely qualitative, and the high level of expertise needed to analyze each item raises questions about its diffusion into clinical practice. Furthermore, in most studies, interobserver and intraobserver variabilities were also not assessed [5]. Another limitation stems from the time-consuming nature of interpretation that might require a postprocedural review of the images, which hampers a real-time decision by the physician. Such an analysis also requires training because of an extended learning curve [6]. Therefore, there is still a major unmet need for a simplified system of quantitative image analysis by endomicroscopy.

Accurate IBD diagnosis is crucial in order to provide a personalized treatment, medical as well as surgical. In particular, because 10% to 15% of cases of chronic colitis are unclassified, discriminating between Crohn's disease (CD) and ulcerative colitis (UC) cases is a major issue in patients needing surgery. However, IBD diagnosis, surveillance and treatment rely on a wide number of parameters, including clinical and endoscopic evaluation as well as histology, serology, and radiology [7–9] that hamper the development of simple diagnostic criteria. Among the most important parameters, mucosal histological evaluation of acute and chronic inflammatory cell infiltrates, crypt abscesses, mucin depletion, epithelial lining integrity and crypt architectural irregularities are currently used to diagnose IBD and help to differentiate CD from UC cases [10,11]. In this context, the use and analysis of "virtual biopsies," such as those obtained from CLE images, could be of major interest to increase the speed of analysis and to reduce sampling errors inherent to the limited mucosal area analyzed. Ultimately, CLE might help not only to target biopsies in order to perform a differential diagnosis between CD and UC cases in indeterminate colitis patients[12] but also to predict disease evolution[13], monitor response to treatment [14] and screen for residual inflammation in macroscopically normal mucosa of treated patients [15,16]. Furthermore, parameters gained with CLE, such as the shape of the crypts, microvascular alteration and fluorescein leakage, have been identified [17], and scores have been proposed to predict relapse and/or assess residual inflammatory activity of IBD [3,4,18,19]. However, these scores are based on semi-quantitative observer-dependent analysis of images, and therefore, creating novel methods and scores allowing diagnosis in IBD is needed. In this context, we herein report a computer-based analysis of CLE data that allows for the diagnosis of IBD and, additionally, for the differentiation of CD from UC cases.

Methods

Study design and patients

We conducted a retrospective study on all consecutive adult patients who were diagnosed with CD or UC or were screened for colonic cancer (control group) and underwent CLE between 2009 and 2016 at the Gastroenterology Departments of the University Hospital of Nantes and the European Hospital Georges Pompidou of Paris (France) in prior studies [20,21]. The study was recorded under the clinical trial number BRD 08/6-A. The diagnosis of IBD was based on clinical, endoscopic and pathologic data. Selected CD patients were in clinical and endoscopic remission, defined by a Harvey-Bradshaw Index ≤4 at the time of enrollment and a Crohn's disease endoscopic index of severity (CDEIS) ≤3. Selected UC patients were also in clinical and endoscopic remission, defined by a partial clinical Mayo score ≤2 with no individual subscore >1 and by a partial endoscopic Mayo score of 0 or 1 at the time of enrollment. Patients who were undergoing colonoscopy for screening or surveillance of polyps/cancer served as the control group. Demographic data (gender, age) and IBD characteristics (age at diagnosis, IBD extension based on the Montreal classification and disease duration) were collected at inclusion. Patients could be secondarily excluded from the study if the CLE video recording quality was insufficient, ie, (1) if the total number of analyzable crypts after mosaicking was less than 35; (2) if the recording was performed in the first 10 minutes or after 20 minutes after fluorescein injection; (3) if the duration of the recording was less than 5 minutes; or (4) if clinical data were missing.

Colonoscopy and probe-based confocal laser endomicroscopy procedures

Polyethylene glycol was used in all patients for colonic preparation. Five physicians with previous experience in CLE performed colonoscopies in sedated patients with high-resolution endoscopes. A dedicated CLE system comprised of a portable laser station (Cellvizio) and an endoscopic probe (Coloflex, Mauna Kea Technologies, Paris, France) were used to perform endomicroscopy. The endoscopy nurse injected intravenously 5ml of a 10% fluorescein sodium solution in anticipation, then the probe was threaded through the operating channel of the endoscope and positioned onto the colonic mucosa under endoscopic guidance in order for the record to start within 10 and 20 minutes after the fluorescein injection [20]. The choice of colonic areas imaged by CLE was left to the endoscopist's discretion, as all patients were in endoscopic remission.

Software, programs and calculations

To analyze a large surface, recordings were first investigated with the Cellvizio Viewer software (Mauna Kea Technologies, Paris, France) to perform mosaicking, which consisted of stitching consecutive frames to “rebuild” the surface covered by the probe. Each mosaic was then processed to measure 14 parameters that were used to perform a quantitative analysis of the mucosa, hereafter referred to as “cryptometry.”

After the mosaic was obtained, intrinsic architectural parameters of the crypts were calculated using the Icy software (Institut Pasteur, Paris, France) [22]. To perform the calculation, we used the active cells plug-in that implements an active contour segmentation method, using exponential splines as basic functions to represent the outline of the crypt, which computes a region of interest. The corresponding geometric data were thus obtained using the region of interest statistics tool, ie, the perimeter, the sphericity, the roundness, the maximal Feret diameter, the elongation factor and the ratio of the maximal axis to minimal axis.

Concerning the crypt density measurement, we have developed a macro in ImageJ (U.S. National Institutes of Health, Bethesda, Md, USA) [23] software to calculate the ratio between the field of view area and the sum of the areas of the crypt. The measurement of the minimal and mean intercrypt distance and wall thickness have been adapted from a plug-in [24].

The vessel parameters were measured using the IC Viewer (Mauna Kea Technologies, Paris, France) version 3.8.6 Vessel Detection plug-in. This plug-in enabled an automatic detection of the vessels directly from each endomicroscopic recording frame, based on fluorescence intensity detection with a threshold set manually at 10 µm. We reported the vessel lengths and areas to the field of view area to normalize the data.

Finally, the fluorescein leakage through the colonic mucosa (FLCM), defined by the increase of mucosal fluorescence over time, was measured using the “signal analysis” tool of the Cellvizio Viewer software. Because the Cellvizio confocal endomicroscopic probe in the clinical version requires internal calibration, we could not directly compare the fluorescence intensity between patients. Thus, we calculated the FLCM as the increase in fluorescence intensity reported in time units, independent from the calibration.

Study outcomes

One functional parameter, FLCM, was analyzed as well as 13 morphological parameters, which were as follows (Figure 1):

Morphological aspect of the crypts:

- Perimeter;
- Sphericity, defined by 4 x π x Area / Perimeter², expressed as a percentage;
- Roundness, defined by the normalized ratio between radii of the minimum and maximum circles inside the crypt shape, expressed as a percentage;
- Maximal Feret diameter (named Feret), defined by the maximal distance between 2 points of the perimeter;
- Elongation factor, defined by the ratio between the minor diameter and the major diameter;
- Ma/ma ratio, defined by the ratio between the width and the height of the box containing the crypt;
- Density, defined by the ratio of the crypt area and the area of the field of view.

Vasculature:

- The mean vessel area, defined by the ratio of the vessels area and the area of the field of view;
- The mean vessel length;
- The mean vessel diameter.

Surface epithelium:

- The minimal and the mean distance between the geometrical centers of neighboring crypts, i.e., intercrypt distance (ICD);
- Wall thickness, defined by the distance between nearest neighbor crypts.

To account for the surface irregularity, we evaluated the coefficient of variation, i.e., the relative measure of data dispersion around the mean, using the percentage of each parameter [25]. We assumed that a significant variation in the values could be indicative of a greater surface irregularity.

The measured outcomes were the comparison of these parameters: (1) between the control and IBD patients and (2) between the Crohn's disease (CD) and ulcerative colitis (UC) patients and (3) the construction of diagnosis scores.

Statistical analysis

Statistical analyses were performed using the GraphPad Prism software (GraphPad Prism 5.0, GraphPad Software Inc). The mean comparisons were performed using the non-parametric Mann-Whitney test. The area under the receiver operating characteristic curve (AUROC), the multivariate regression and the logistic model were performed using STATA 14 (Stata Corp LP). Differences with a *P* value less than .05 were considered statistically significant.

Results

Patients

Sixty-one IBD patients and 9 control patients were screened. The clinical and demographic data are detailed in Table 1. Eleven patients were excluded: 3 because of insufficient video quality or crypt number and 8 because of missing clinical data (Figure 2). Among the 23 CD patients, the disease was mostly ileo-colonic (78%) and was non-stricturing and non-penetrating in 13 (57%) patients. Among the 27 UC patients, 6 (22%) had a disease limited to the rectum, 16 (60%) had a left-sided colitis, and 5 (18%) had a pancolitis. The mean disease duration was similar for CD and UC patients, 15±7 and 16±10 years (p=0.720), respectively. No adverse event associated with fluorescein injection was noted.

Mucosal cryptometry of controls and IBD patients

We retrospectively analyzed 438 CLE movies from IBD patients and 20 CLE movies from control patients, which represented a surface of 665±100 mm²/control, 1505±185 mm²/CD and 1642±137 mm²/UC. An average of 228±115 and 153±76 crypts was analyzed in the IBD group and control group, respectively (Figure 3). Movies recorded 20 min after the fluorescein injection and movies for which mosaics could not have been automatically generated were excluded from the analysis. In IBD patients, the crypt perimeter, the Feret diameter, the mean intercrypt distance, the wall thickness and the FLCM were significantly increased compared to control patients by 126%

(p=0.0159), 140% (p=0.0027), 155% (p<0.0001), 188% (p<0.0001) and 297% (p=0.0057), respectively. Except for the sphericity and the density of the crypt, all coefficients of variation (example in Figure 4A) were increased in IBD patients compared to control patients (Table 2).

Specific mucosal cryptometry of CD and UC patients

With the purpose of identifying discriminant parameters between CD and UC, we compared the parameters previously described between CD and UC. We analyzed a mean number of 230±124 and 226±110 crypts per patient in the CD and the UC groups, respectively.

Concerning the distribution of the crypts, in UC patients, the mean and minimal ICD as well as the wall thickness and FLCM were significantly increased by 109% (p=0.0211), 111% (p=0.0079), 117% (p=0.0032), and 174% (p=0.0051), respectively, compared to CD patients. In addition, the elongation factor and the mean vessel length were significantly decreased by 7% (p=0.0493) and 12% (p=0.0275), respectively, in UC patients compared with CD patients. The coefficient of variation analysis revealed a larger distribution of density values (p=0.0048) and a smaller distribution of wall thickness values (p=0.0070) in UC patients compared with CD patients (Table 2).

Mucosal cryptometry could be used as a marker of IBD

The area under the receiver operating characteristic curve (AUROC) was calculated for each parameter and coefficient of variation to evaluate first their power of discrimination between control patients and IBD patients (Table 3). Using a univariate regression analysis, we identified the coefficient of variation of the maximal Feret diameter (COV_{Feret}) as the most powerful parameter to discriminate between control patients and IBD patients, with an AUROC of 98%. Next, we applied a multivariate logistic regression of COV_{Feret} on the other parameters. The addition of COV_{Feret} to the wall thickness (**WT)** or to the mean ICD increased the AUROC to 100%. Then, we aimed to construct a score that would allow us to separate the IBD patients from the control patients using a logistic model that included COV_{Feret} and WT. This score, named IBDiag, was calculated as follows:

IBDiag=-361.498+13.42*$\mathbf{COV_{Feret}}$+0.590***WT**

In the control patients, IBDiag is always <0, whereas in the IBD patients, IBDdiag is always >0 (Figure 4B) (100% [93%;100%] sensitivity and 100% [66%;100%] specificity).

Following the same rationale, we performed a univariate AUROC and a multivariate logistic regression (Table 4) with the CD and UC groups. The WT was the most powerful feature to discriminate between CD patients and UC patients, with an AUROC of 74.4%. The multivariate logistic regression using WT required 7 parameters (wall thickness, FLCM, $COV_{WallThickness,}$ $COV_{MeanVesselArea,}$ $COV_{Perimeter,}$ minimal ICD and mean vessel length) to increase the AUROC to 97.16%.

Next, we aimed to construct a score that would allow us to discriminate between CD patients and UC patients using a logistic model (**IBDif**=-24.520+0.123*__FLCM__- 0.400+$\mathbf{COV_{WT}}$ +0.138*$\mathbf{COV_{MeanVesselArea}}$ +0.194*$\mathbf{COV_{Perimeter}}$+0.066*__Minimal ICD__+653.943*__Mean Vessel Length).__

This score allowed the calculation of the probability to properly diagnose UC rather than CD patients as follows:

$$\mathbf{P_{UC}} = e^{IBDif} / (1-e^{IBDif})$$

IBDif allowed discriminating UC from CD patients with a sensitivity of 92.3% [75%;99%] and a specificity of 91.3% [72%;99%]. The probability cut-off between UC and CD patients is illustrated in Figure 4C. The probability of making the right diagnosis then increased exponentially with either the sensitivity for UC patients or the specificity for the CD patients. When this method is used, only two patients in each group would have been misclassified.

Discussion

In the present study, we demonstrated that CLE images could differentiate normal endoscopic mucosa between healthy controls and patients with IBD and between patients with CD and UC. We were able to quantitatively assess changes in the CLE morphology of the crypts' pit pattern, vessels and fluorescence into colonic mucosa and to construct predictive scores that discriminated between IBD and control patients and between patients with CD and UC.

The first major finding of our study was to identify various parameters, such as the crypt perimeter, the Feret diameter, the mean intercrypt distance, the wall thickness and the FLCM that were significantly increased in IBD patients compared to control patients. Such alterations reflect changes in the mucosal architecture that have been previously reported to be altered in IBD [19,26,27]. In particular, Kiesslich et al [4] showed that fluorescein leakage observed in the ileum was one of the parameters that could predict relapse of both UC and CD. Another study reported a correlation between the severity of UC and changes in crypt architecture as well as fluorescein

leakage [14]. In addition to changes in the absolute value of the parameters, our study showed that most coefficients of variation were increased in IBD patients compared to control patients, most likely highlighting the heterogenicity of mucosal lesions in IBD.

An important finding of our study is that we were able to identify single parameters that discriminated between CD and UC patients. In particular, the increase in FLCM in UC patients compared to CD patients might reflect an increased vascular permeability in UC patients, which is a parameter that had not been assessed in a study comparing UC and CD patients [12]. Conversely, the reduced vascular length observed in UC versus CD patients is concordant with vascular alterations described in previous UC studies [3,15,17]. Some of the discriminative parameters between CD and UC patients reported in our study were also identified by Tontini et al [12]. For example, we report an increased intercrypt distance in UC patients, which is concordant with the decreased crypt density described in their study. The discrepancy between UC and CD changes seen by CLE could be a consequence of the predominant superficial lesions in UC (including mucosal edema and neoangiogenesis associated with increased FLCM) compared to a most transmural disease in CD. In the same way, it has been demonstrated that mucosal histological normalization of colon biopsies impacts the prognosis of UC contrary to CD. One could hypothesize that deeper histological modifications not accessible with forceps could also have an impact on the prognosis of CD. However, these modifications could also not be detected by CLE explaining the discrepancies between UC and CD.

Another interesting aspect of our study, linked to the analysis of quantitative parameters, was that we were able to develop quantitative scores that allowed discriminating with high accuracy between IBD and control patients and, even more importantly, between UC and CD patients. To our knowledge, no score has previously been devised to differentiate between IBD and control patients using CLE. Among scores that have been developed to assess inflammation using CLE [3,16,19,27] or predict relapse [4,18,28], only one aimed at discriminating CD versus UC patients. Indeed, Tontini et al. proposed the IDEA score that distinguished CD and UC patients [12]. This score was calculated from observations of the CLE images by expert operators on a cohort of IBD patients and was based on descriptive features such as architectural distortion, surface irregularity or crypt density. In contrast, the IBDif score has the advantage of being automated and designed using quantitative parameters.

The major advantage of our study was that we developed a simple and automated image analysis procedure allowing the quantitative analysis of CLE images. This automated analysis method provides major advantages over previous studies by reducing the time of analysis, the interobserver error and the learning curve. In an attempt to determine the learning curve of a CLE score, a study reported a quick improvement in agreement between experienced and inexperienced analysts for determining the score over time [6]. However, the different subparts of the score were all based on qualitative features and did not provide similar agreement. Endoscopists must frequently master new skills due to constant improvements in imaging technology, especially in high-definition endoscopy; therefore, the need to learn CLE features definitely hampers its application in routine practice. Studies suggest that such training can be efficiently done, but the learning curve is clearly an obstacle. Our work demonstrates that computer-based measurements are easy and have the capacity to remove CLE from the hands of the experts. In future studies, a comparison between human and computer analysis would be of great interest.

The main limitation of this study stems from its retrospective nature, which might have created a bias in the selection of patients and in the data collection. In addition, as the procedure has been developed from already classified patients, the relevance of the identified IBD markers in this study must be validated in future studies. On the other hand, an advantage of the retrospective nature of this study was that the data analysis was made years after the data acquisition, and therefore, we were able to check on the last known status of the patients and confirm that no patient had changed from their initial diagnosis of either CD or UC. Another limitation of this study was that it was conducted on a subset of homogeneous IBD patients, ie, in clinical remission. Therefore, it remains to be validated whether the different scores developed also apply in different populations, such as IBD patients in an active phase, treatment-naïve patients or symptomatic patients with normal endoscopic findings. The selection of movies according to their quality may also have introduced a bias but was imperative to the analysis as it relies completely on mosaicking. Another limitation of our analysis stems from the use of multiples computer programs to obtain the measurements. However, if the interest of this analysis is confirmed in other studies, these programs could be combined in order to facilitate and accelerate the process. Indeed, the study of the crypts is already partly automated in contrast to the calculation of FLCM and the analysis of the vessels. A software model allowing the integration of the 4 current steps of analysis (crypts, relationship between the crypts, FLCM and vessels) could be built for

post-processing analysis. However, in order to perform real-time analysis, the software solution would have to be integrated to the endomicroscopy laser station.

In conclusion, our findings suggest that computer-based analysis of CLE images has a high potential for the development of in vivo diagnosis of digestive diseases. Whether computed analysis is superior to image analysis by the endoscopist remains to be determined in future studies. These results, especially the diagnostic accuracy of the analysis, need to be confirmed in large-size prospective studies before clinical implementation of computer-based analysis of CLE images.

Reference list

1. Kiesslich R, Burg J, Vieth M, *et al.* Confocal laser endoscopy for diagnosing intraepithelial neoplasias and colorectal cancer in vivo. *Gastroenterology* 2004 ; 127 : 706–713.

2. Kiesslich R, Gossner L, Goetz M, *et al.* In vivo histology of Barrett's esophagus and associated neoplasia by confocal laser endomicroscopy. *Clin. Gastroenterol. Hepatol. Off. Clin. Pract. J. Am. Gastroenterol. Assoc.* 2006 ; 4 : 979–987.

3. Li C-Q, Xie X-J, Yu T, *et al.* Classification of inflammation activity in ulcerative colitis by confocal laser endomicroscopy. *Am. J. Gastroenterol.* 2010 ; 105 : 1391–1396.

4. Kiesslich R, Duckworth CA, Moussata D. Local barrier dysfunction identified by confocal laser endomicroscopy predicts relapse in inflammatory bowel disease. *Gut* 2012 ; 61 : 1146–1153.

5. Karstensen JG. Evaluation of confocal laser endomicroscopy for assessment and monitoring of therapeutic response in patients with inflammatory bowel disease. *Dan. Med. J.* 2016 ; 63 .

6. Chang J, Ip M, Yang M, *et al.* The learning curve, interobserver, and intraobserver agreement of endoscopic confocal laser endomicroscopy in the assessment of mucosal barrier defects. *Gastrointest. Endosc.* 2016 ; 83 : 785-791.e1.

7. Van Assche G, Dignass A, Panes J, *et al.* The second European evidence-based Consensus on the diagnosis and management of Crohn's disease: Definitions and diagnosis. *J. Crohns Colitis* 2010 ; 4 : 7–27.

8. Dignass A, Eliakim R, Magro F, *et al.* Second European evidence-based consensus on the diagnosis and management of ulcerative colitis Part 1: Definitions and diagnosis. *J. Crohns Colitis* 2012 ; 6 : 965–990.

9. Soubières AA, Poullis A. Emerging role of novel biomarkers in the diagnosis of inflammatory bowel disease. *World J. Gastrointest. Pharmacol. Ther.* 2016 ; 7 : 41–50.

10. Bressenot A, Peyrin-Biroulet L. Histologic features predicting postoperative Crohn's disease recurrence. *Inflamm. Bowel Dis.* 2015 ; 21 : 468–475.

11. Marchal Bressenot A, Riddell RH, Boulagnon-Rombi C, *et al.* Review article: the histological assessment of disease activity in ulcerative colitis. *Aliment. Pharmacol. Ther.* 2015 ; 42 : 957–967.

12. Tontini GE, Mudter J, Vieth M, *et al.* Confocal laser endomicroscopy for the differential diagnosis of ulcerative colitis and Crohn's disease: a pilot study. *Endoscopy* 2015 ; 47 : 437–443.

13. Karstensen JG, Săftoiu A, Brynskov J, *et al.* Confocal laser endomicroscopy: a novel method for prediction of relapse in Crohn's disease. *Endoscopy* 2016 ; 48 : 364–372.

14. Karstensen JG, Săftoiu A, Brynskov J, *et al.* Confocal laser endomicroscopy in ulcerative colitis: a longitudinal study of endomicroscopic changes and response to medical therapy (with videos). *Gastrointest. Endosc.* 2016 ; 84 : 279-286.e1.

15. Macé V, Ahluwalia A, Coron E, *et al.* Confocal laser endomicroscopy: a new gold standard for the assessment of mucosal healing in ulcerative colitis. *J. Gastroenterol. Hepatol.* 2015 ; 30 Suppl 1 : 85–92.

16. Chang J, Leong RW, Wasinger VC, *et al.* Impaired Intestinal Permeability Contributes to Ongoing Bowel Symptoms in Patients With Inflammatory Bowel Disease and Mucosal Healing. *Gastroenterology* 2017 ; 153 : 723-731.e1.

17. Maione F, Giglio MC, Luglio G, *et al.* Confocal laser endomicroscopy in ulcerative colitis: beyond endoscopic assessment of disease activity. *Tech. Coloproctology* 2017 ; 21 : 531–540.

18. Buda A, Hatem G, Neumann H, *et al.* Confocal laser endomicroscopy for prediction of disease relapse in ulcerative colitis: A pilot study. *J. Crohns Colitis* 2014 ; 8 : 304–311.

19. Neumann H, Vieth M, Atreya R, *et al.* Assessment of Crohn's disease activity by confocal laser endomicroscopy. *Inflamm. Bowel Dis.* 2012 ; 18 : 2261–2269.

20. Wallace MB, Meining A, Canto MI, *et al.* The safety of intravenous fluorescein for confocal laser endomicroscopy in the gastrointestinal tract. *Aliment. Pharmacol. Ther.* 2010 ; 31 : 548–552.

21. Mahfouz E, Rahmi G, Canard J-J. Résultats de l'observatoire national des pratiques de l'endomicroscopie confocale par minisonde (ou Cellvizio®). Abstract JFHOD 2017

22. Chaumont F de, Dallongeville S, Chenouard N, *et al.* Icy: an open bioimage informatics platform for extended reproducible research. *Nat. Methods* 2012 ; 9 : 690–696.

23. Schneider CA, Rasband WS, Eliceiri KW. NIH Image to ImageJ: 25 years of image analysis. *Nat. Methods* 2012 ; 9 : 671–675.

24. Haeri M, Haeri M. ImageJ Plugin for Analysis of Porous Scaffolds used in Tissue Engineering. *J. Open Res. Softw.* 2015 ; 3.

25. Magro F, Langner C, Driessen A, *et al.* European consensus on the histopathology of inflammatory bowel disease. *J. Crohns Colitis* 2013 ; 7 : 827–851.

26. Watanabe O, Ando T, Maeda O, *et al.* Confocal endomicroscopy in patients with ulcerative colitis. *J. Gastroenterol. Hepatol.* 2008 ; 23 Suppl 2 : S286-290.

27. Musquer N, Coquenlorge S, Bourreille A, *et al.* Probe-based confocal laser endomicroscopy: A new method for quantitative analysis of pit structure in healthy and Crohn's disease patients. *Dig. Liver Dis. Off. J. Ital. Soc. Gastroenterol. Ital. Assoc. Study Liver* 2013.

28. Hundorfean G, Chiriac MT, Mihai S, *et al.* Development and Validation of a Confocal Laser Endomicroscopy-Based Score for In Vivo Assessment of Mucosal Healing in Ulcerative Colitis Patients. *Inflamm. Bowel Dis.* 2017 ; 24 : 35–44.

Acknowledgement:

E Coron, T Matysiak-Budnick, M Le Rhun, A Bourreille and N Musquer performed the CLE of patients included in this study.

Figure legends

Figure 1: Cryptometry parameters

a, Perimeter defined by 4 x π x Area / Perimeter²**; b, Maximal Feret diameter** defined by the maximal distance between 2 points of the perimeter**; c, Sphericity; d, Roundness** defined by the normalized ratio between radii of the minimum and maximum circles written in the form**; e, Elongator factor** defined by the ratio between the minor diameter and the major diameter**; f, Ma/ma ratio** defined by the ratio between the width and the height of the box containing the crypt**; g, Density** defined by the ratio of the crypt area and the area of the field of view**; h, Wall Thickness** defined by the distance between nearest neighbor crypts**; i,** Minimal and mean distance between the geometrical centers of neighbor crypts**; j, Mean vessel area** defined by the ratio of the vessels area and the area of the field of view.

Figure 2: Flow chart

Figure 3: Examples of Confocal Laser Endomicroscopy (CLE) mosaics.

A: Colonic mucosa of a control subject displaying round regular crypts with regular distance and normal vascularization. B: CLE mosaics of colonic mucosa in an IBD patient displaying distorted crypts with uneven diameters and irregular intercrypt spaces

Figure 4: Graphical representation of the distribution of roundness values, IBDiag score and PUC probability.

A: Coefficient of variation of the roundness parameter in controls and patients with inflammatory bowel disease, expressed as a percentage

B: Values of the IBDiag score in controls and patients with inflammatory bowel disease.

C: Values of the probability to properly diagnose UC rather than CD (PUC) in IBD patients

Table 1: Subjects' characteristics

	Controls	Crohn's Disease	Ulcerative Colitis
n	9	23	27
Age, mean (min-max), years	58 (29-79)	40 (18-74)[a]	50 (22-71)
Sex, n (M/F)	7/2	13/10	15/12
Disease duration, median, years (IQ)	NA	15±6	17±10.5
Crohn's disease phenotype, n (%) (Classification)			
Non stricturing, non-penetrating	NA	13 (57)	NA
Stricturing	NA	7 (30)	NA
Penetrating	NA	3 (13)	NA
Crohn's disease location, n (%)			
Ileal	NA	1 (4)	NA
Colonic	NA	3 (13)	NA
Ileo-colonic	NA	18 (78)	NA
Upper gastrointestinal tract	NA	1 (4)	NA
Perineal[(1)]	NA	7 (30)	NA
Crohn's disease clinical activity (Harvey Bradshaw Index), median (95% IC)	NA	0 (0-1)	NA
Crohn's disease endoscopic activity (CDEIS), median (95% IC)	NA	2 (0-6)	NA
Ulcerative colitis location, n (%)			
Proctitis	NA	NA	6 (22)
Left-sided colitis	NA	NA	14 (52)
Extensive colitis	NA	NA	2 (8)
Pancolitis	NA	NA	5 (18)
Ulcerative colitis clinical activity (CAI), median (95% IC)	NA	NA	0 (0.1-0.5)
Ulcerative colitis endoscopic activity (Mayo score), median (95% IC)	NA	NA	0.5 (0-1)
History of surgery[(2)]	NA	5 (22)	0 (0)
Treatment received at the time of endoscopy, n (%)			
Salazopyrine	NA	7 (30)	13 (48)
Budesonide	NA	2 (9)	0 (0)
Methotrexate	NA	1 (4)	0 (0)
Azathioprine	NA	6 (26)	4 (14)
Anti TNF	NA	5 (22)	8 (30)
Other[(3)]	NA	2 (9)	2 (8)

(1) None of the patients had only perineal or upper GI location

(2) Ileo-caecal resection in 4/5 cases

(3) 2 patients were naïve of any treatment; 2 patients received Cyclosporine or Tacrolimus

a (p=0.0063) one-way ANOVA with the Dunn post-test for comparison of control patients and Crohn's disease patients.

Table 2: Cryptometry of different groups (control patients, overall IBD patients, CD patients and UC patients)

ICD: intercrypt distance; FLCM: fluorescein leakage through the colonic mucosa; COV: coefficient of variation.

* p<0.05: comparison of control and IBD

** *P*< .05: comparison of CD and UC

	Control		Inflammatory Bowel Disease		Crohn's disease		Ulcerative colitis	
	Mean (± S.D.)	COV (± S.D.) %	Mean (± S.D.)	COV (± S.D.) %	Mean (± S.D.)	COV (± S.D.) %	Mean (± S.D.)	COV (± S.D.) %
Perimeter (µm)	594.1 (± 211.4)	13.66 (± 4.39)	748.1 (± 163.5)*	28.60 (± 13.69)*	765.2 (± 137.1)	26,3 (± 10.3)	733.5 (± 163.5)	30.5 (± 16.0)
Sphericity (%)	97.29 (± 2.40)	3.34 (± 4.09)	95.08 (± 3.52)	5.39 (± 4.29)	95.0 (± 3.4)	5,8 (± 4.1)	95.1 (± 3.7)	5.1 (± 4.5)
Roundness (%)	73.83 (± 11.88)	13.24 (± 2.96)	68.10 (± 12.20)	22.77 (± 9.81)*	66.5 (± 11.8)	23,5 (± 8.8)	69.4 (± 12.6)	22.2 (± 10.7)
Max Feret diameter (µm)	194.9 (± 80.0)	13.43 (± 2.25)	273.3 (± 65.9)*	29.26 (± 11.41)*	281.0 (± 73.0)	27,9 (± 9.0)	265.0 (± 59.6)	30.4 (± 13.2)
Elongation Factor	1.27 (± 0.14)	13.10 (± 2.84)	1.40 (± 0.18)	23.12 (± 9.16)*	1.45 (± 0.18)	24,7 (± 8.9)	1.36 (± 0.16)**	21.8 (± 9.3)
Major axis / minor axis	1.204 (± 0.116)	11.84 (± 4.10)	1.254 (± 0.090)	18.82 (± 6.65)*	1.28 (± 0.08)	20,1 (± 6.1)	1.23 (± 0.09)	17.7 (± 7.0)
Density	0.238 (± 0.052)	27.80 (± 15.39)	0.314 (± 0.120)	41.60 (± 20.41)	0.335 (± 0.100)	34,6 (± 8.9)	0.296 (± 0.133)	47.6 (± 25.2)**
Mean Vessel Length	0.018 (± 0.003)	17.94 (± 7.04)	0.017 (± 0.003)	41.55 (± 36.89)*	0.018 (± 0.003)	33,4 (± 9.6)	0.016 (± 0.003)	39.7 (± 19.9)
Mean Vessel Area	0.233 (± 0.041)	19.13 (± 7.24)	0.213 (± 0.039)	44.09 (± 52.14)*	0.233 (± 0.041)	34,9 (± 10.8)	0.203 (± 0.039)	34.5 (± 11.1)
Mean Vessel Diameter (µm)	13.01 (± 0.88)	8.69 (± 1.97)	12.47 (± 0.72)	11.46 (± 2.29)*	12.6 (± 0.8)	12,0 (± 2.7)	12.4 (± 0.7)	11.0 (± 1.8)
Mean ICD µm)	316.7 (± 93.6)	17.29 (± 3.63)	492.5 (± 70.1)*	27.60 (± 4.64)*	468.3 (± 78.4)	27,8 (± 4.1)	513.0 (± 55.6)**	27.4 (± 5.1)
Minimal ICD (µm)	253.1 (± 66.2)	17.31 (± 4.11)	280.5 (± 37.4)	25.27 (± 5.22)*	264.8 (± 37.2)	24,6 (± 3.7)	293.9 (± 32.5)**	25.8 (± 6.3)
Wall thickness (µm)	170.4 (± 66.1)	34.19 (± 8.33)	321.5 (± 65.37)*	43.54 (± 6.85)*	294.4 (± 69.5)	45,8 (± 6.5)	344.6 (± 52.6)**	41.6 (± 6.7)**
FLCM	7.17 ± (4.62)	N.A.	21.27 (± 14.50)*	N.A.	15.2 (± 8.3)	N.A.	26.5 (± 16.7)**	N.A.

Table 3: Univariate and multivariate ROC analyses of controls and IBD patients.

The coefficient of variation of the maximal Feret diameter (bold) was the most powerful parameter to discriminate control from IBD patients. The addition of COV_{Feret} to the wall thickness or to the mean ICD increased the AUROC to 100%.

ICD: intercrypt distance; FLCM: fluorescein leakage through the colonic mucosa; COV: coefficient of variation.

Parameter	Univariate AUROC	Multivariate AUROC (Parameter+COV_{Feret})
Perimeter	71.33	98.00
Sphericity	72.44	97.78
Roundness	65.56	98.00
Feret	79.22	98.44
Elongation factor	74.44	98.00
Ma/ma	68.00	98.22
Density	70.44	98.22
Mean Vessel Length	59.18	97.96
Mean Vessel Area	65.65	97.73
Mean Vessel Diameter	67.35	98.41
Mean ICD	96.89	100.00
Minimal ICD	56.00	98.22
Wall Thickness	96.67	100.00
FLCM	86.89	99.11
$COV_{Perimeter}$	92.44	98.67
$COV_{Sphericity}$	75.78	98.67
$COV_{Roundness}$	89.56	98.44
COV_{Feret}	**98.00**	
$COV_{Elongation\ factor}$	88.00	98.22
$COV_{Ma/ma}$	81.11	98.00
$COV_{Density}$	74.89	98.00
$COV_{Mean\ Vessel\ Length}$	89.33	98.44
$COV_{Mean\ Vessel\ Area}$	84.67	98.44
$COV_{Mean\ Vessel\ Diameter}$	81.33	99.33
$COV_{mean\ ICD}$	96.89	99.33
$COV_{minimal\ ICD}$	88.89	98.89
$COV_{WallThickness}$	80.89	97.78

Table 4: Univariate and multivariate ROC analyses of Ulcerative Colitis and Crohn's Disease groups. The multivariate logistic regression from the wall thickness requires 7 parameters (bold) to increase the AUROC to 97.16% to discriminate ulcerative colitis from Crohn's Disease.

ICD: intercrypt distance; FLCM: fluorescein leakage through the colonic mucosa; COV: coefficient of variation.

Parameter	Univariate AUROC	Multivariate AUROC						
		+ Wall Thickness	+ FLCM	+ COV Wall Thickness	+ COV Mean Vessel Area	+COV Perimeter	+ Minimal ICD	+ Mean Vessel Length
Perimeter	63.29	74.56	81.16	85.83	88.08	91.95	95.81	95.81
Sphericity	53.38	74.40	80.84	86.96	88.57	90.50	93.56	93.56
Roundness	59.98	74.24	81.00	85.51	87.44	91.95	94.69	94.69
Feret	63.77	73.91	81.48	85.99	88.08	92.59	95.65	95.65
Elongation factor	66.26	74.72	81.96	85.83	88.41	93.24	95.17	95.17
Ma/ma	65.30	73.11	81.16	85.67	87.76	92.59	94.36	94.36
Density	65.54	74.72	80.19	85.67	88.08	90.34	93.72	93.72
Mean Vessel Length	68.39	78.26	84.45	87.46	89.63	93.65	**97.16**	
Mean Vessel Area	64.97	76.92	82.27	87.46	89.80	92.64	96.49	96.49
Mean Vessel Diameter	60.20	74.58	80.60	84.62	87.12	90.64	93.48	93.48
Mean ICD	69.08	76.01	80.52	86.31	88.24	90.98	94.36	94.36
Minimal ICD	71.98	73.11	82.61	87.76	88.89	**93.72**		
Wall Thickness	74.40							
FLCM	72.06	**80.52**						
$COV_{Perimeter}$	54.27	77.62	81.64	87.92	**90.50**			
$COV_{Sphericity}$	57.49	75.04	80.19	85.51	87.76	93.24	95.49	95.49
$COV_{Roundness}$	60.63	74.72	80.19	86.15	87.28	92.11	94.85	94.85
COV_{Feret}	52.50	76.65	81.96	87.60	90.02	91.63	94.04	94.04
$COV_{Elongation\ factor}$	60.63	73.43	81.00	85.83	87.76	92.11	94.20	94.20
$COV_{Ma/ma}$	60.95	73.43	80.84	85.99	87.76	92.11	94.20	94.20
$COV_{Density}$	73.35	77.46	82.93	88.41	89.86	93.56	95.97	95.97
$COV_{Mean\ Vessel\ Length}$	52.74	75.36	80.52	88.24	88.24	90.02	93.56	93.56
$COV_{Mean\ Vessel\ Area}$	49.44	75.04	80.84	**88.57**				
$COV_{Mean\ Vessel\ Diameter}$	60.87	79.23	83.74	87.92	89.53	93.40	95.81	95.81
$COV_{mean\ ICD}$	55.23	75.20	85.19	86.15	88.08	90.50	93.72	93.72
$COV_{Minimal\ ICD}$	54.43	73.43	80.35	87.28	88.89	91.30	95.17	95.17
$COV_{Wall\ thickness}$	72.30	76.97	**85.67**					

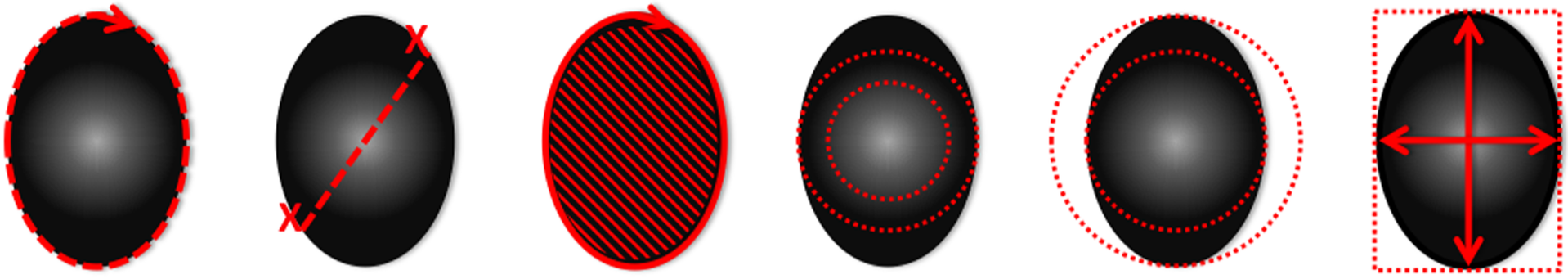

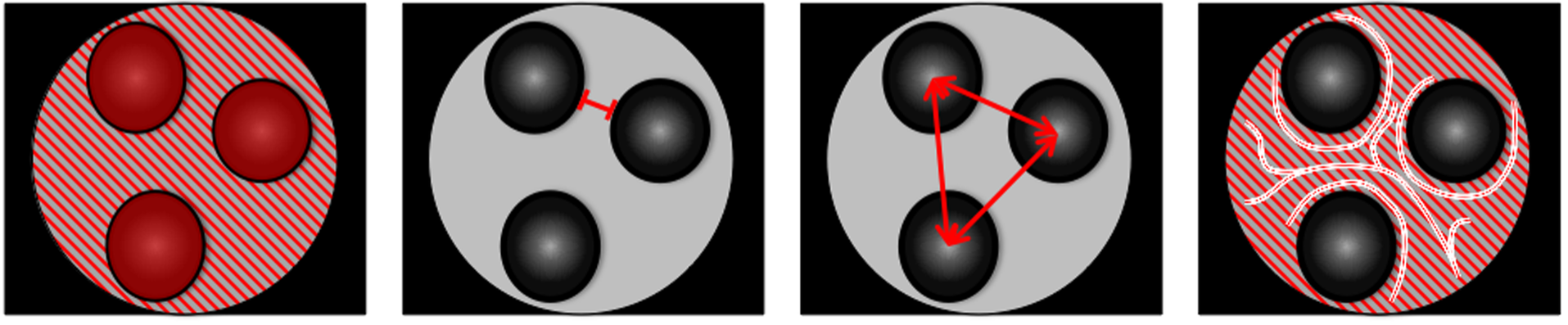

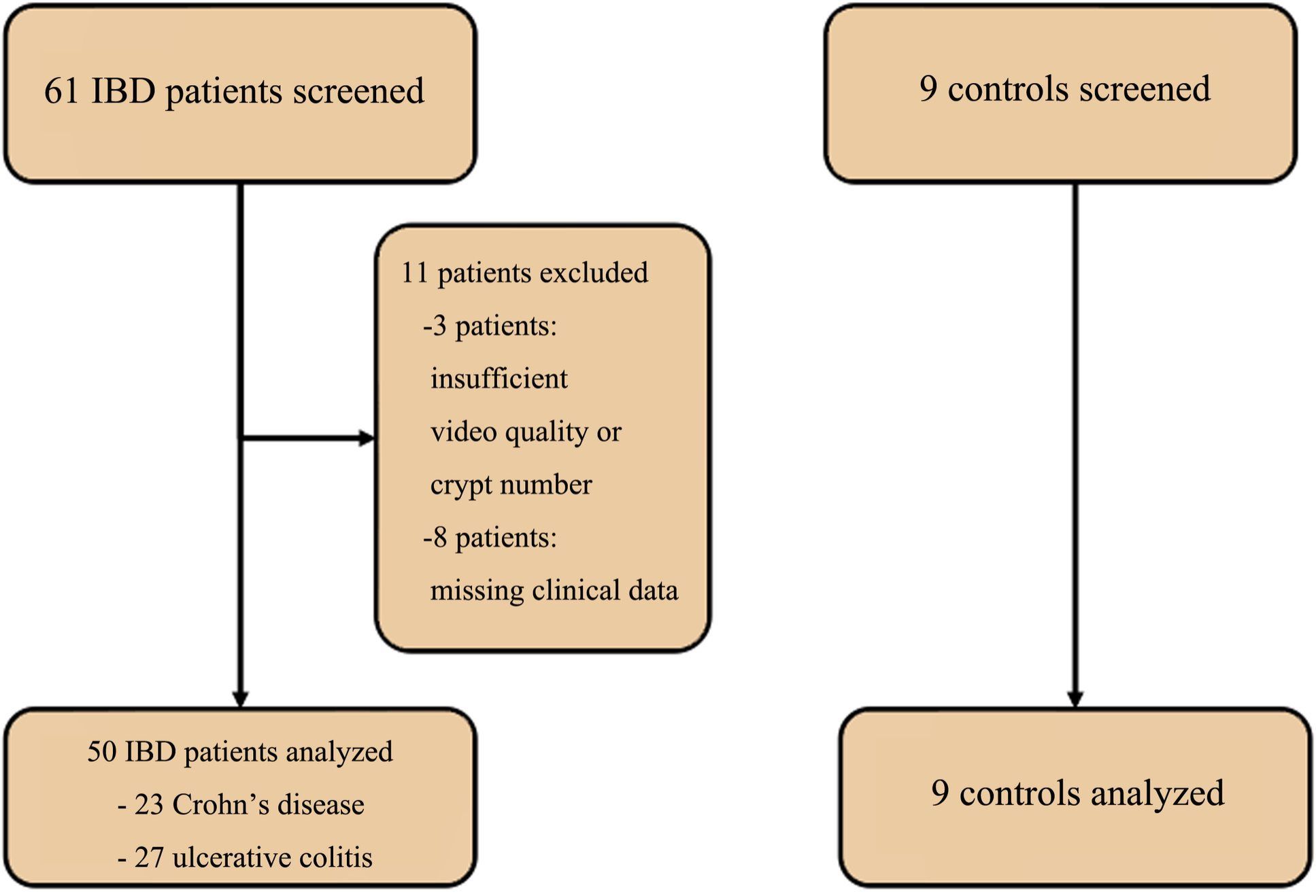
61 IBD patients screened
9 controls screened
11 patients excluded
-3 patients:
insufficient
video quality or
crypt number
-8 patients:
missing clinical data
50 IBD patients analyzed
- 23 Crohn's disease
- 27 ulcerative colitis
9 controls analyzed

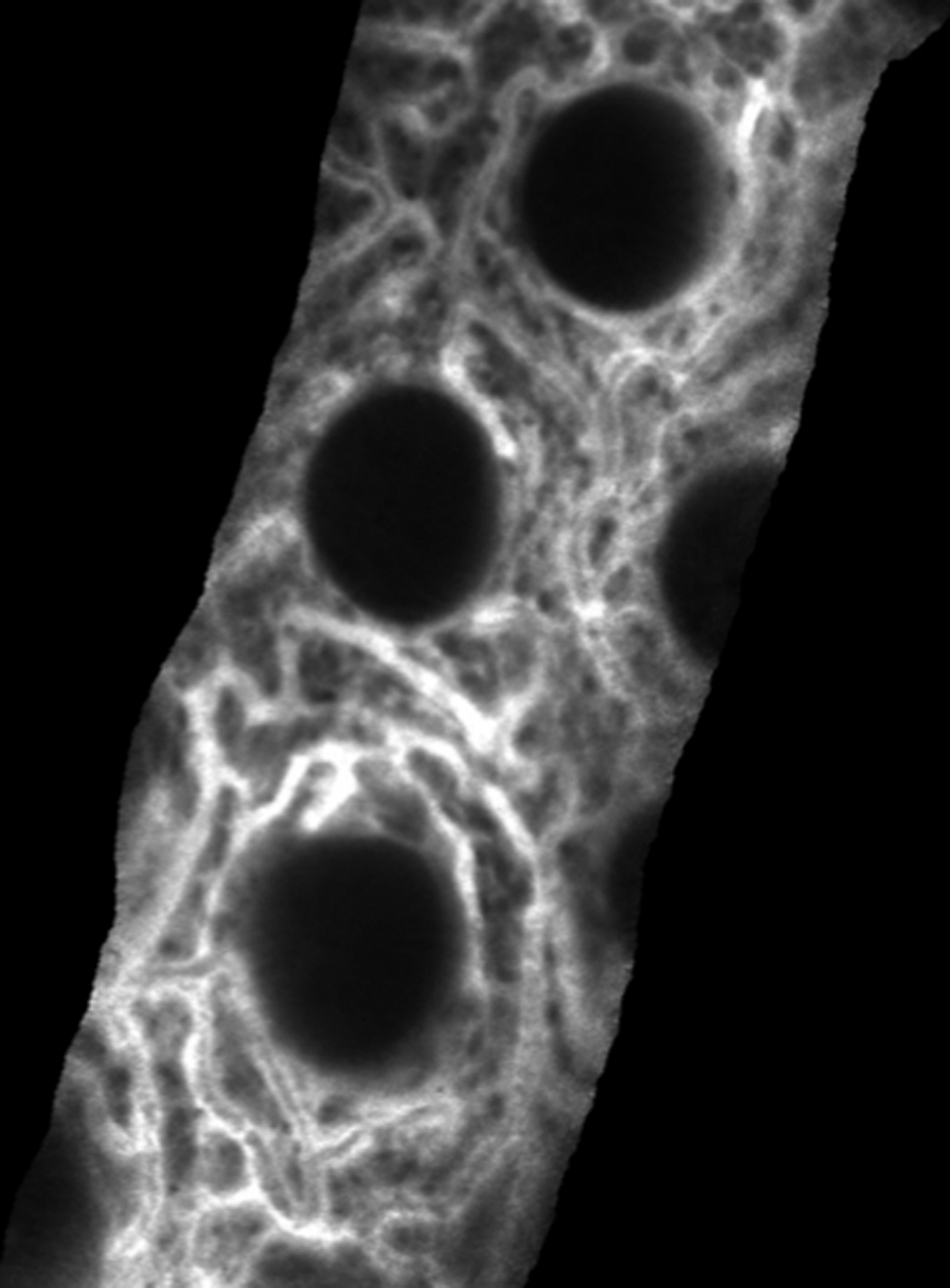

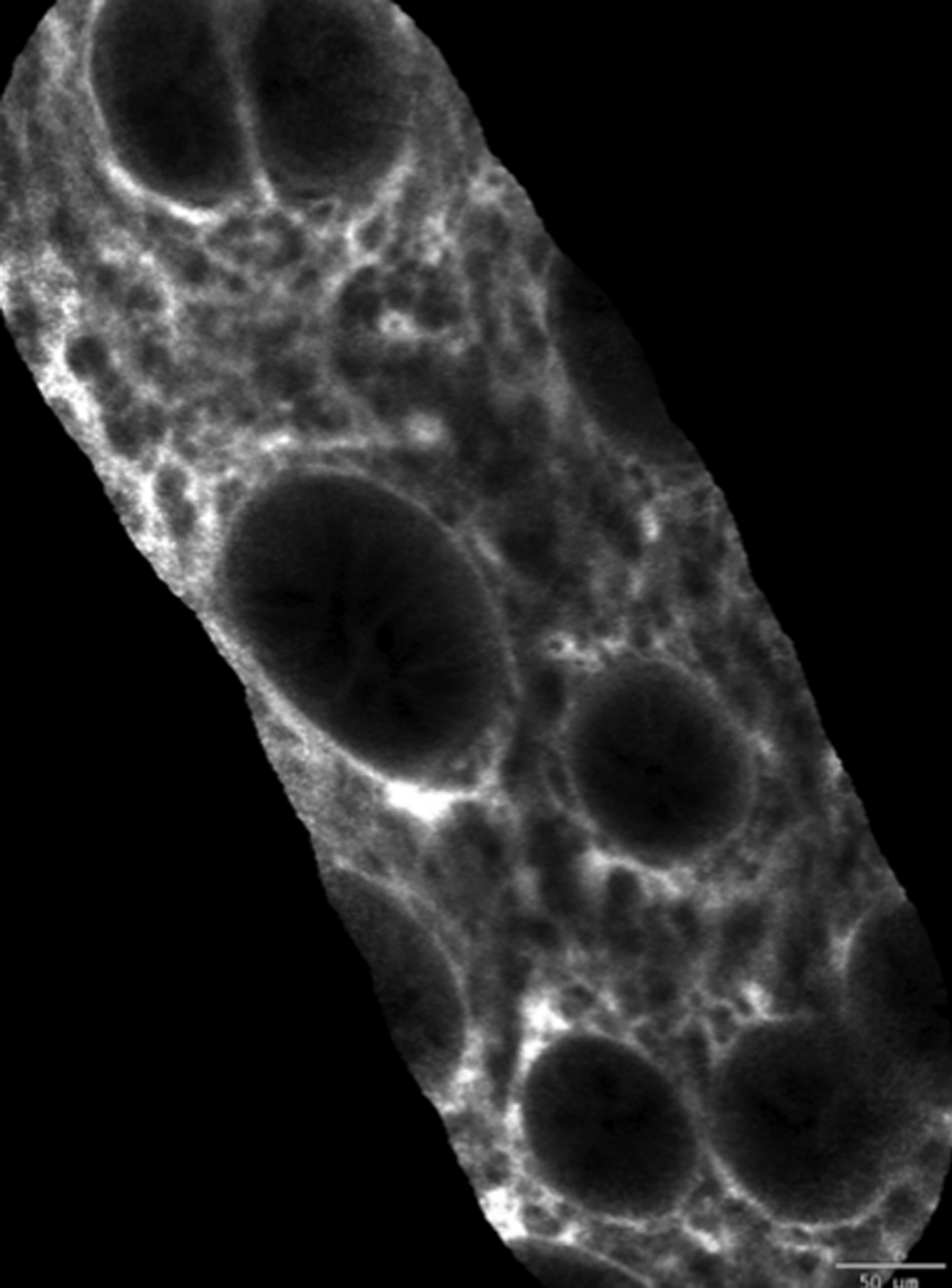
50 µm

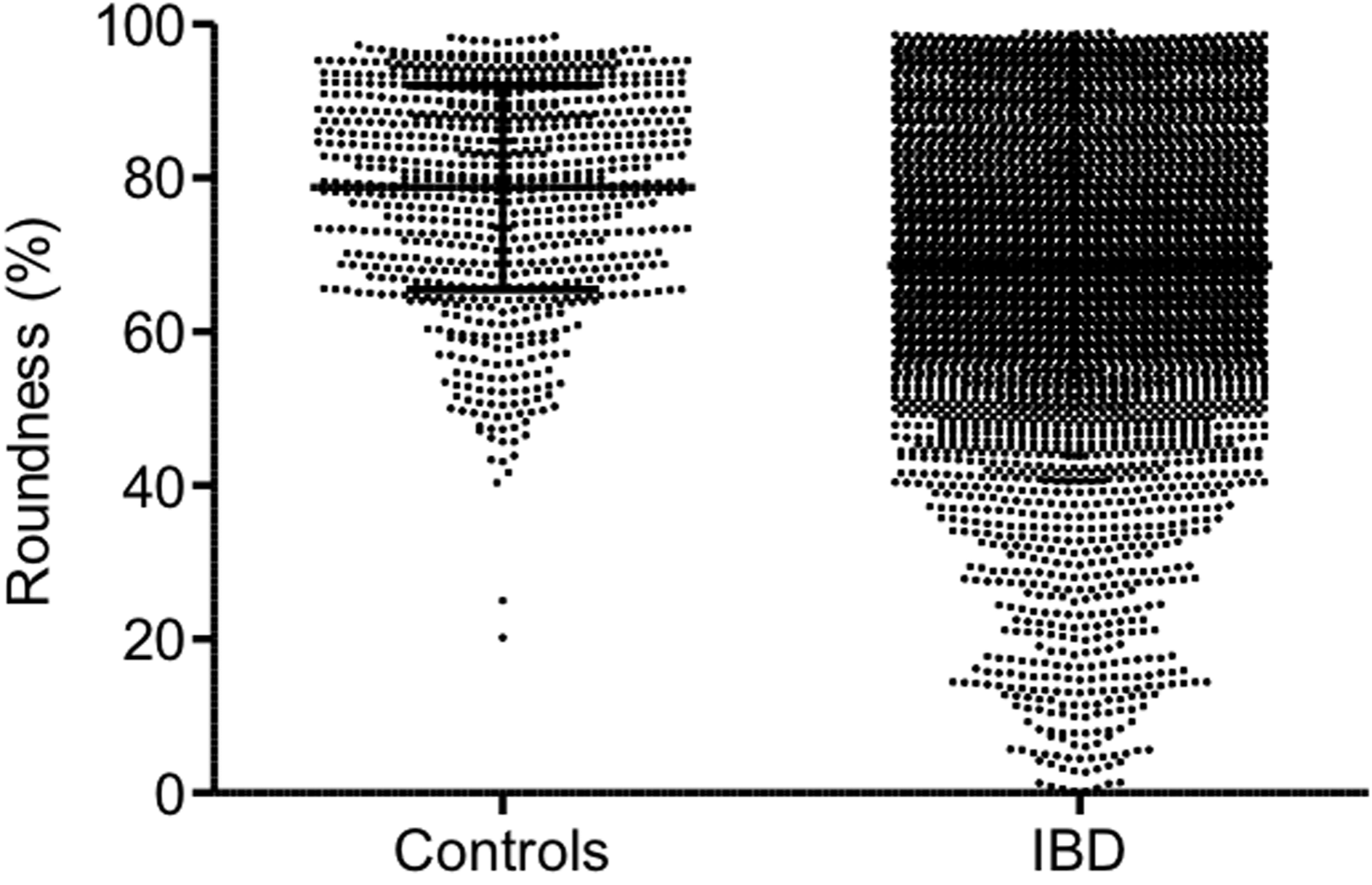
100
80
60
40
20
0
Roundness (%)
Controls
IBD

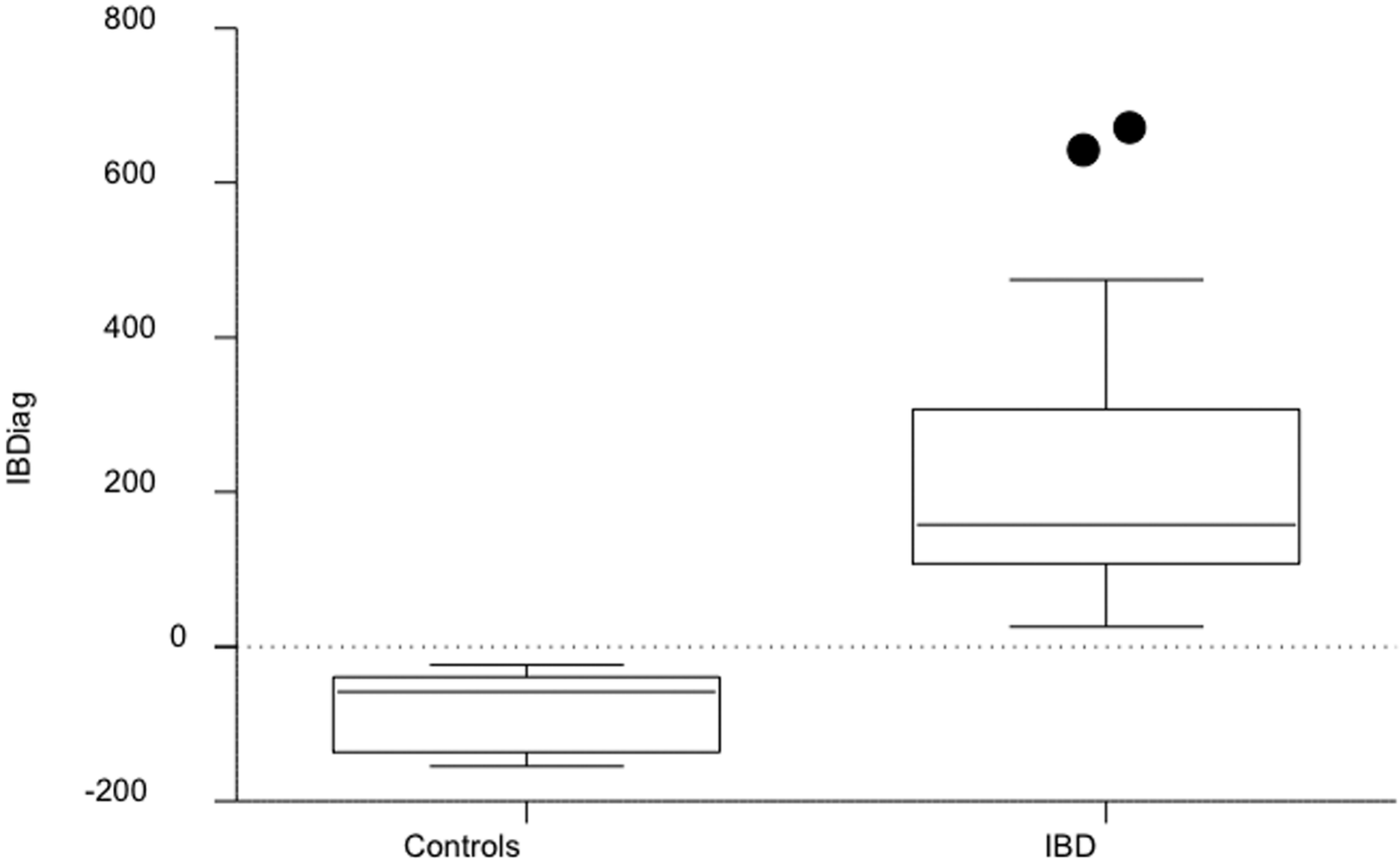
800
600
400
200
0
-200
IBDiag
Controls
IBD

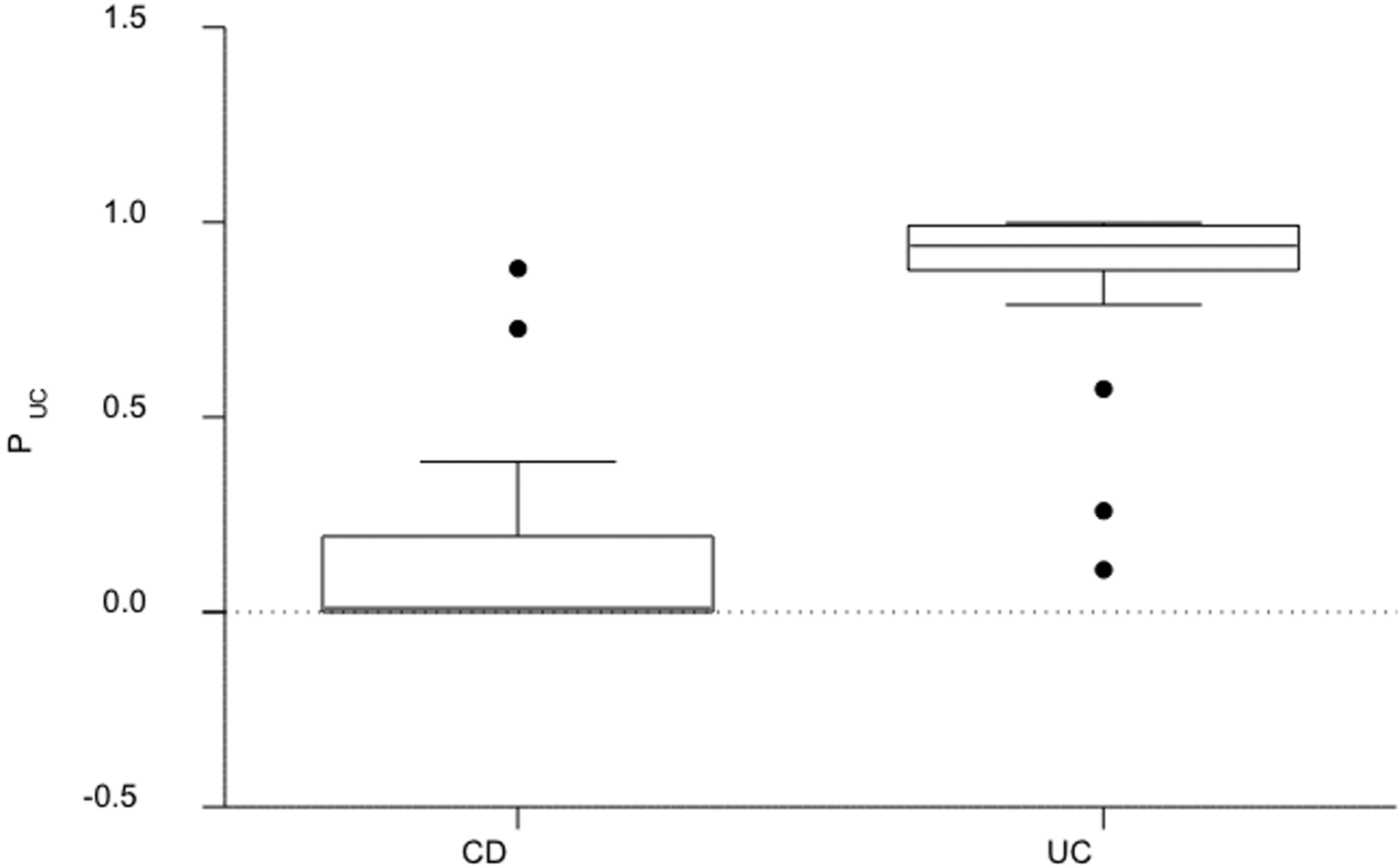
1.5
1.0
0.5
0.0
-0.5
P UC
CD
UC